Peer-reviewed version available at *Geosciences* **2018**, *8*, 354; doi:10.3390/geosciences8090354

Characterizing a Naturally-Fractured Carbonate Formation for a CO_2 Storage Operation

Yann Le Gallo (1), José Carlos de Dios (2)

(1) Geogreen, Rueil Malmaison, France (ylg@geogreen.fr),
(2) Fundación Ciudad de la Energía, Cubillos del Sil, Spain, (jc.dedios@ciuden.es)

Abstract

Investigation into geological storage of CO_2 is underway at the Technology Development Plant (TDP) at Hontomín (Burgos, Spain), the only current onshore injection site in the European Union. The storage reservoir is a deep saline aquifer located within Low Jurassic Formations (Lias and Dogger), formed by fractured carbonates with low matrix permeability. Understanding the processes involved in CO_2 migration within this kind of low-primary permeability carbonates influenced by fractures and faults is key to ensure safe operation and reliable plume prediction. During the hydraulic characterization tests, 2300 tons of liquid CO_2 and 14000 m^3 of synthetic brine were co-injected on site in various sequences to characterize the pressure response of the seal-storage pair [de Dios et al, 2017]

The injection tests were analyzed with a compositional dual media model which accounts for both temperature effects (as the CO_2 is liquid at the bottom of the wellbore) and multiphase flow hysteresis (to effectively simulate the alternating brine and CO_2 injection tests that were performed). The pressure and temperature responses of the storage formation were history-matched mainly through the petrophysical characteristics of the fracture network [Le Gallo et al, 2017]. The dynamic characterization of the fracture network dominates the CO_2 migration while the matrix does not appear to significantly contribute to the storage capacity.

This initial modeling approach was improved using the characterization workflow developed within the European FP7 CO2ReMove project for sandstone fractured reservoirs [Ringrose et al., 2011; Deflandre et al., 2011]. Fractured reservoirs are challenging to handle because of their high level of heterogeneity that conditions the reservoir behaviour during the injection. In particular, natural fractures have a significant impact on well performance [Ray et al, 2012]. Furthermore, the understanding of the processes involved in CO_2 migration within relatively low-permeability storage influenced by fractures and faults is essential for enabling safe storage operation [Iding and Ringrose, 2010].

As part of the European H2020 ENOS project, the site geological model is updated by integration of the recently acquired data such as the image log interpretations from injection and observation wells.

The geological model is generated through the analysis and integration of data including borehole images and well test data.

Following a methodology developed for naturally fractured hydrocarbon reservoirs [Ray et al., 2012], the image log analysis identified two sets of diffuse fractures. A Discrete Fracture Network [Bourbiaux et al., 2005] was built around both wells which encompass the caprock, storage and underburden formations.

The fracture characteristics of the two sets of diffuse fractures, such as orientations, densities and conductivities, are calibrated upon the interpretation of the injection tests [Le Gallo et al, 2017]. For each facies, the DFN characteristics were then upscaled and propagated to the full-field reservoir simulation model as 3D fracture properties (fracture porosity, fracture permeability and equivalent block size).

Keywords: CO_2 geological storage, fractured carbonates, CO_2 migration plume, updated geological model, Discrete Fracture Network

Introduction

CO_2 geological storage has reached industrial scale in sites such as Sleipner (Norway), In-Salah (Algeria), and Decatur (USA). These sites represent examples approaching the ideal conditions for establishing a commercial site according to criteria established in SACS project [Chadwick et al. 2007]. Other CO_2 injection pilots also achieved notable scientific results for example including Otway (Australia), Ketzin (Germany), Nagaoka (Japan), Lacq (France) [Kovács et al, 2015].
The Hontomín pilot is the only current onshore injection site in Europe for CO_2 geological storage, recognized by the European Parliament [EP resolution 2014] as key test facility for CCS technology development. It is located close to Burgos in the north of Spain, owned by Fundación Ciudad de la Energía (CIUDEN).
The Hontomin storage reservoir comprises fractured limestones and dolomites .The injection of CO_2 into fractured carbonate rocks for dedicated storage is unique in a European context, although considerable experience of injection into carbonates was gained in North America in association with enhanced oil recovery operations as for example in the Weyburn oil field [Whittaker et al, 2011].

Prior to dynamic modeling the CO_2 migration, a detailed modeling of the characteristics of the storage complex is required as a key first step workflow for CO_2 storage site characterization [Delprat-Jannaud et al., 2015]. This paper presents the main features of the geological model with its stratigraphic and petrophysical properties. This work integrates the characterization (size, conductivities) of the natural fracture networks by its modeling in the vicinity of the wells [de Joussineau et al, 2016].

Geological context

The storage site represents a structural dome where the cap rock and reservoir belong to the Jurassic formations Marly Lias and Sopeña respectively. Keuper is the underlying seal and Dogger, Purbeck and Weald form the overburden [Rubio et al 2014]. The representative lithological column of Hontomín site and geological cartography of the area are shown in the Figure 1.

Preprints (www.preprints.org) | NOT PEER-REVIEWED | Posted: 23 May 2018 doi:10.20944/preprints201805.0324.v1

Peer-reviewed version available at Geosciences 2018, 8, 354; doi:10.3390/geosciences8090354

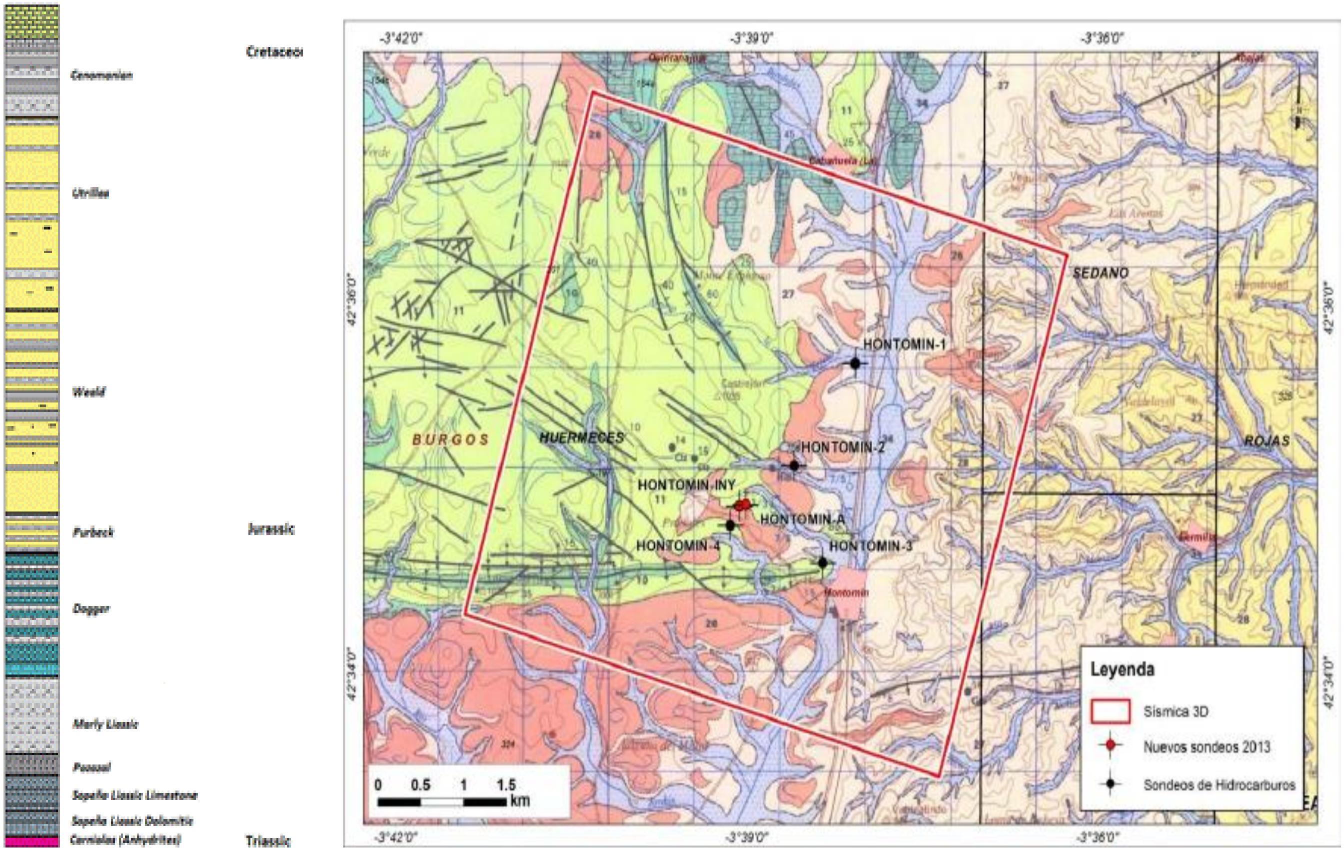

Figure 1. Lithological column and geological cartography of Hontomín area

The Marly Lias and Pozazal formations are mainly comprised of highly carbonated marls (close to 50%) with uniaxial strength values equal or higher than 130 MPa and Young Modulus values in the range 15-30 GPa. The Sopeña formation is comprised of limestone in the upper part of reservoir and dolomite at the bottom. Their geomechanical properties correspond to rocks with high values of uniaxial strength, as the cap rock case, being the values for limestone and dolomite equal or higher than 180 MPa and 190 MPa respectively. As regards the Young modulus values, they are in the ranges of 30-60 GPa and 50-85 GPa [Kovács, 2014].

These data suggest that there are different post fracture behaviors for the seal and reservoir, taking into account the tectonic effects induced in the rock layers during the formation of the dome. Uniaxial strength values are really high for a carbonated marl, but the Young modulus range reveals that despite being a strong rock its behavior should be of type “strain softening”, with relevant deformations pre and post fracture. On other hand, carbonates (limestone and dolomite) show also high values of uniaxial strength, but Young modulus values support the behavior should be of type “elastic brittle” that means no significant strains take place after rock fracture.

According to mentioned assumptions, Hontomín geological model covers two different fault groups which affect the reservoir and overburden respectively, but there is no continuity between them through the cap rock what ensures its integrity, except two cases described below. Figure 2 shows the arrangement of faults and fractures in the study area.

Peer-reviewed version available at *Geosciences* **2018**, *8*, 354; doi:10.3390/geosciences8090354

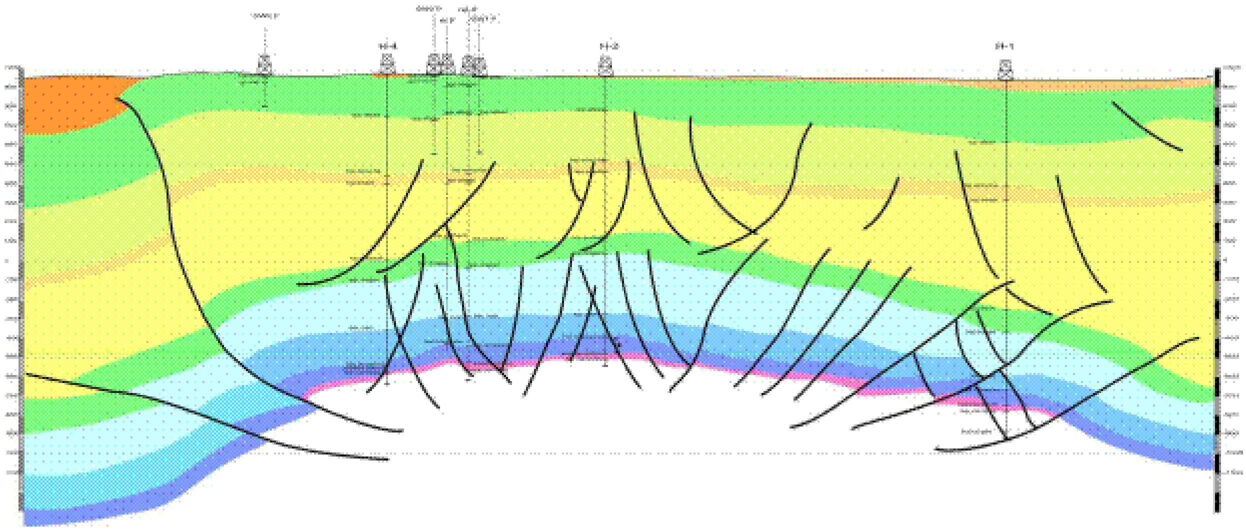

Figure 2. Faults and fractures within reservoir and overburden at Hontomín site

On the other hand, the values of some petrophysical properties determined by laboratory tests, as effective porosity, gas permeability and injections of CO_2 and brine in reservoir conditions to assess the hydrodynamic and geochemical effects, revealed that fluid transmissivity is dominated by carbonate fractures, while the matrix does not appear to significantly contribute to the storage capacity. Results from subsequent tests conducted at field scale on site during the hydraulic characterization phase supported this assumption [de Dios et al, 2017].

Two main faults cross the storage complex from the reservoir to the overburden, which are considered limits in the geological model. Ubierna fault, located at the southern part of Hontomín area, and East fault are shown in Figure 3. Future works will be carried out to determine if both faults are sealing or transmissible to flow.

Peer-reviewed version available at *Geosciences* **2018**, *8*, 354; doi:10.3390/geosciences8090354

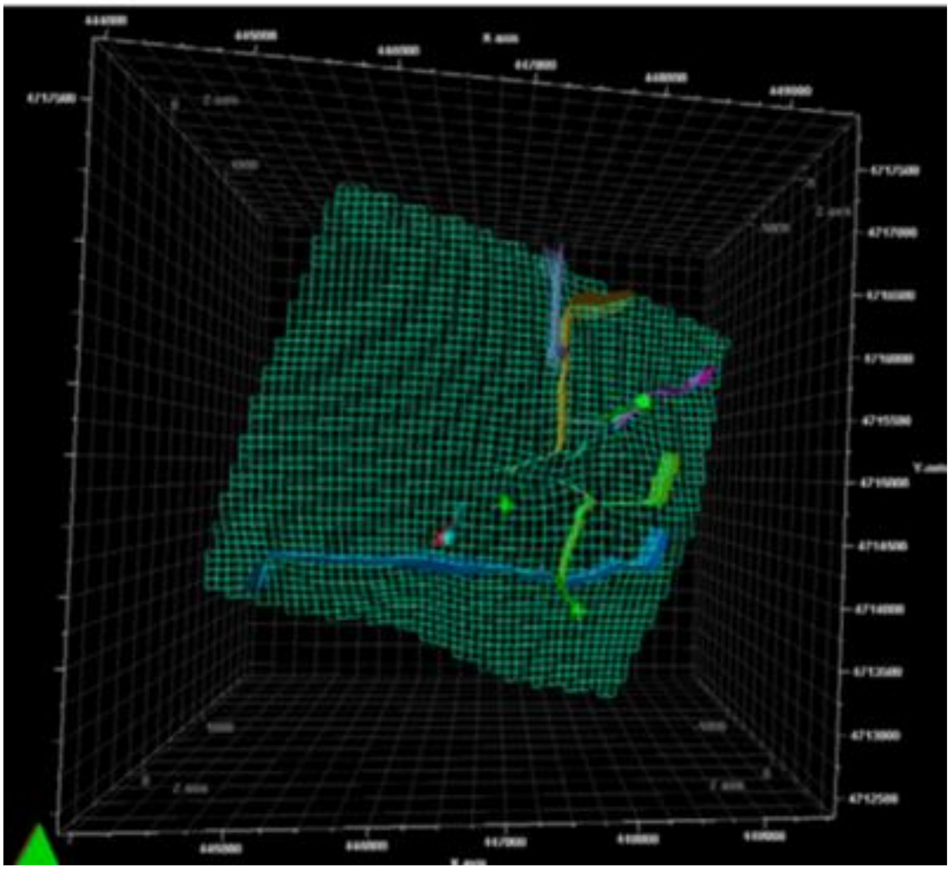

Figure 3. South (Ubierna) and East faults are limits of Hontomín geological model

Two wells were specifically drilled and monitored during site construction reaching the depth of 1600 m, one for injection (HI) and other for observation (HA) [de Dios et al, 2016]. Four legacy wells are also located in the study area (H1, H2, H3 and H4).

Geological model

The geological model covers the whole storage complex from the overburden (Dogger formation) down to the storage (Sopeña formation) and the underburden (Keuper formation) as shown in Figure 1

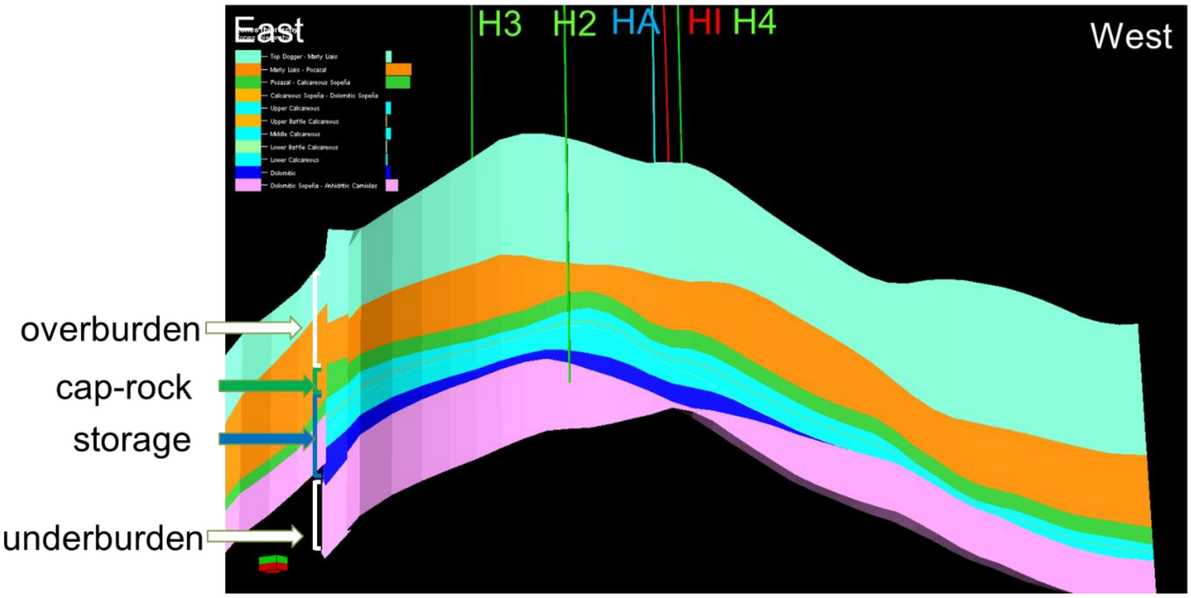

Preprints (www.preprints.org) | NOT PEER-REVIEWED | Posted: 23 May 2018 doi:10.20944/preprints201805.0324.v1

Peer-reviewed version available at *Geosciences* **2018**, *8*, 354; doi:10.3390/geosciences8090354

Figure 1.Vertical cross-section of the geological model of the Hontomìn storage complex; The HA and HI wells are the observation and CO_2 injection wells respectively while H2 to H4 wells are legacy wells

Structural model

A 3-D seismic reflection survey was acquired in 2010 which parameters included 22 source lines (crosslines), deployed E-W, perpendicular to 22 receiver lines (inlines) deployed N-S, with intervals of 25 m between sources and between receivers; the inline and crossline spacing was 250 m and 275 m, respectively, covering a total extent of 36 km^2 [Alcalde et al., 2014]. Due to the complex geological setting of the Hontomìn site and the existence of an unexpected sharp velocity inversion near the surface, associated to the Upper-Lower Cretaceous contact [Alcalde et al., 2014], the 3-D seismic only identified the main horizons below the Dogger. These horizons were matched to the corresponding makers for legacy and newly-drilled wells.
The faults are only interpreted at the top of the storage formation from the 3-D seismic interpretations and are assumed to be vertical.
The grid of the geological model was designed to follow the facies vertical heterogeneities. The lateral heterogeneities representation are coarser due to lack of well correlations.

Petrophysical model

The petrophysical model is established upon the facies and porosity log available from HA and HI wells and laboratory results. Since only the two newly-drilled wells have facies and porosity information, a simple modeling approach is selected for property modeling.

Facies

The vertical correlation length of the facies is assumed to be a function of the formation thicknesses. This is particularly important in the Pozazal, Marly Lias formations which show successions of shale, limestone and marls. The vertical correlation length may alter the vertical connectivity. Consequently, the grid thickness is quite small in the Pozazal formation which shows alternances of marl and shale (see Figure 4).

Porosity

The porosity is distributed within the grid based upon a moving average algorithm from the up-scaled porosity at the newly-drilled wells ensuring they are constrained to the facies distribution in the grid.

Permeability

The permeability is assumed to be constant per facies. The matrix permeability is mainly available from core measurements [Kovács, 2014; Dávila et al, 2016] which may be complemented for some facies by literature data [Bennion and Bachu, 2007] which is consistent with the core measurements.
The previous dynamic modeling [Le Gallo et al, 2017] show a minor contribution of the matrix in the history matching of the pressure response. The fracture permeability is the main driver to the history matching of the pressure response [Le Gallo et al, 2017].

Preprints (www.preprints.org) | NOT PEER-REVIEWED | Posted: 23 May 2018 doi:10.20944/preprints201805.0324.v1

Peer-reviewed version available at *Geosciences* **2018**, *8*, 354; doi:10.3390/geosciences8090354

The model is populate in terms of facies, porosity and permeability as shown in Figure 2

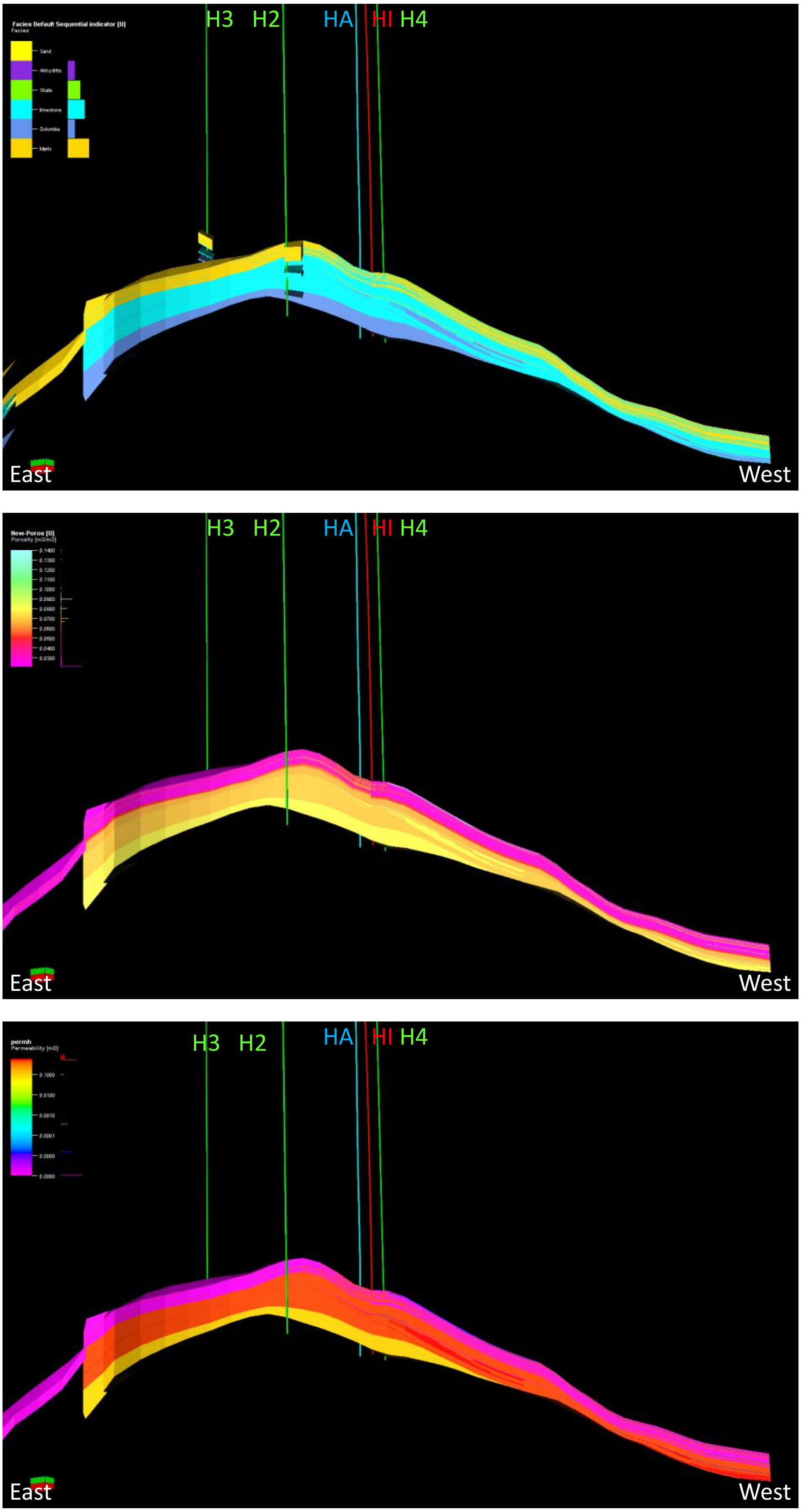

Peer-reviewed version available at Geosciences 2018, 8, 354; doi:10.3390/geosciences8090354

Figure 2.Vertical cross-section of the facies (top), porosity (middle) and permeability (bottom) of the Hontomìn storage (Sopeña formation);

Fracture characterization and modeling

A study on fractures characteristics in both wells was conducted during the well logging campaigns, which particularly focused on the reservoir strata [de Dios et al, 2017]. Data gained from acoustic televiewer during the performance of these works provided information about the type of fractures and their distribution [Collier and Ridder, 1992].

DFN modeling

As summarized by Jing [Jing, 2003], the DFN method is a special discrete model that considers fluid flow and transport processes in fractured rock masses through a system of connected fractures.
DFN are particularly well suited the applications on characterization of the permeability of fractured rocks and generic studies of fracture influences, and the design of rock engineering works for near-field problems.
The stochastic simulation of fracture systems is the geometric basis of the DFN approach and plays a crucial role in the performance and reliability of the DFN model. The key process is to create PDFs of fracture parameters relating to the densities, orientations and sizes, based on field mapping results using borehole logging data and scanline or window mapping techniques, and generate the realizations of the fractures systems according to these PDFs and assumptions about fracture shape (circular discs, ellipses or polygons).
The approach implemented in FracaFlow™ is based upon a pipe model which represents a fracture as a pipe of equivalent hydraulic conductivity starting at the disc center and ending at the intersections with other fractures, based on the fracture transmissivity, size and shape distributions [Cacas et al, 1990]
To include the fractures identified in the televiewer log, a specialized software, FracaFlow™ [de Joussineau et al, 2016] is used to better integrate the different fractures into the flow model and calibrate their conductivities on the well test interpretations. Depending upon the geological context, different types of objects may be identified at different scales (Diffuse fractures, fault-associated fractures, faults) which may be intercepted by the wells [Ali et al, 2009]. In general, horizontal wells provide the best source of information on the fractures. However, at Hontomìn, all wells including the newly-drilled one are sub-vertical wells.
The approach relies upon a DFN construction from the identified fracture and calibration of the various parameter upon the well tests [Ray et al, 2012]. A fracture is characterized by its attributes such as orientation (dip and strike), length, aperture, and origin or morphology. A fracture set is a group of fractures having similar attributes. The fracture set can be described with the previous attributes and the density of fractures. The fracture characteristics may be associated to the facies generated on the grid.
The grid and its properties (facies, porosity, and permeability) for the matrix, the main horizons (Top Dogger, Top Lias, Top Calcareous Sopeña, and Top Keuper), the fault maps at Top Calcareous Sopeña and the well trajectories and logs (facies, porosity) are imported into FracaFlow™. All the fractures characteristics for HI and HA from televiewer log [de Dios et al, 2017] were also imported as fracture logs (type, dip and azimuth as a function of depth). As shown in Figure 4, 5 types of fractures (0, 10, 14, 16, 18) were identified from the Dogger to the well shoes (Sopena/Carniolas formations).

Preprints (www.preprints.org) | NOT PEER-REVIEWED | Posted: 23 May 2018 doi:10.20944/preprints201805.0324.v1

Peer-reviewed version available at *Geosciences* **2018**, *8*, 354; doi:10.3390/geosciences8090354

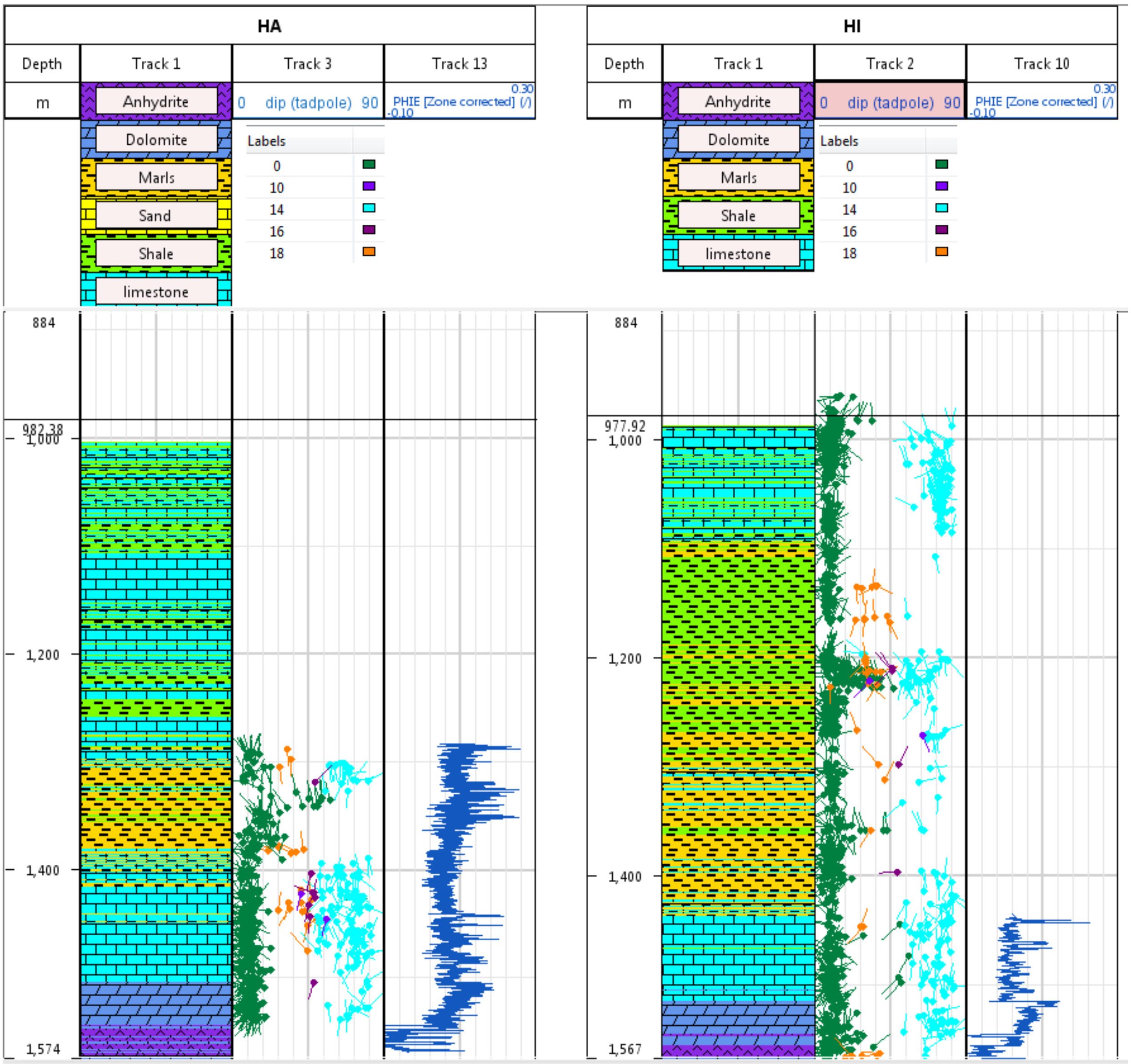

Figure 4 Facies, fracture orientation–televiewer log (Courtesy of ICTJA-CSIC)- and porosity logs for HI and HA

Fracture analysis

The pole analysis is based the statistical analysis of the dip and strike of the fractures. The available fracture may be analyzed based upon the facies which does not allow clear discrimination between the different fracture families.

The pole analysis (Figure 5) is based on the statistical analysis of the dip and strike of the mean pole of each fracture family. The mean poles are analyzed according to their main orientations (dip, strike) as shown in Table 1.

Preprints (www.preprints.org) | NOT PEER-REVIEWED | Posted: 23 May 2018 doi:10.20944/preprints201805.0324.v1

Peer-reviewed version available at Geosciences 2018, 8, 354; doi:10.3390/geosciences8090354

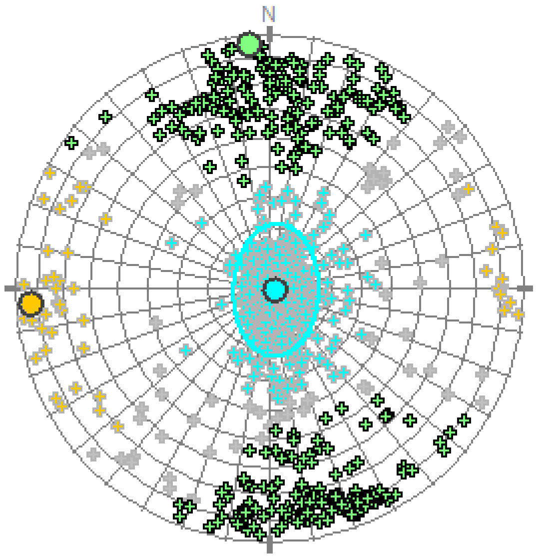

Figure 5 Poles stereo diagram for the bedding (blue), N-S (orange) and E-W (green) fracture families

Table 1 Mean pole of the fracture family as a function of orientation.

Data	Number	Strike(1)	Strike St dev.	Dip(2)	Dip St dev.
E-W	278	85	0,5	84	0,35
N-S	**48**	**176**	**0,3**	**82**	**0,25**

(1) Degree with respect to North

(2) Degree with respect to horizontal

Most of the fractures identified in the wells (Figure 5) represent the factures associated with type '0' which are sub-horizontal and reflects the formation bedding. Two main family of diffuse fractures are identified (Table 1): one with an approximate north/south orientation (strike ~176 N) as shown in Figure 6, one with an approximate East/West orientation (strike ~85N) as shown in Figure 7. They regroup the fractures identified on the televiewer analysis associated with 10, 14, 16, and 18 types from Figure 4.

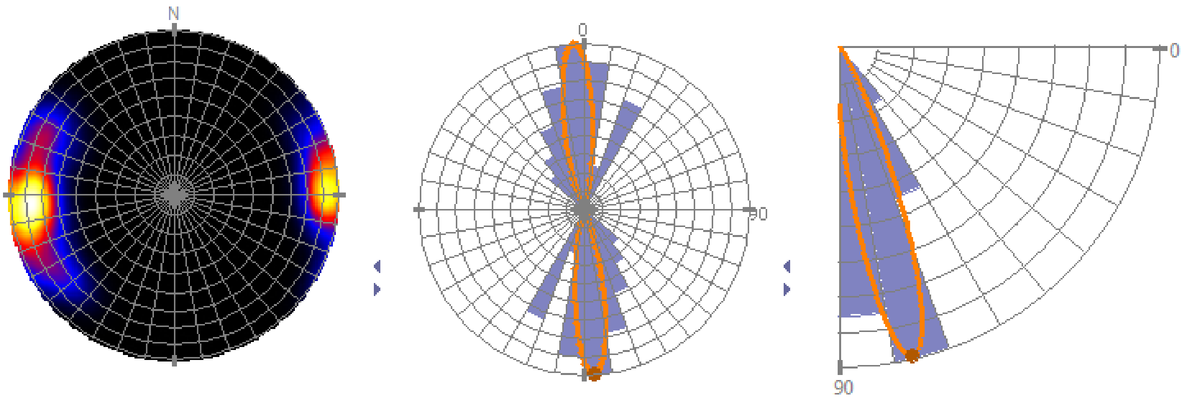

Figure 6 N-S fracture characteristics: fracture density (left), strike (center) and dip (right) diagrams with confidence ellipses for the population mean

Peer-reviewed version available at Geosciences 2018, 8, 354; doi:10.3390/geosciences8090354

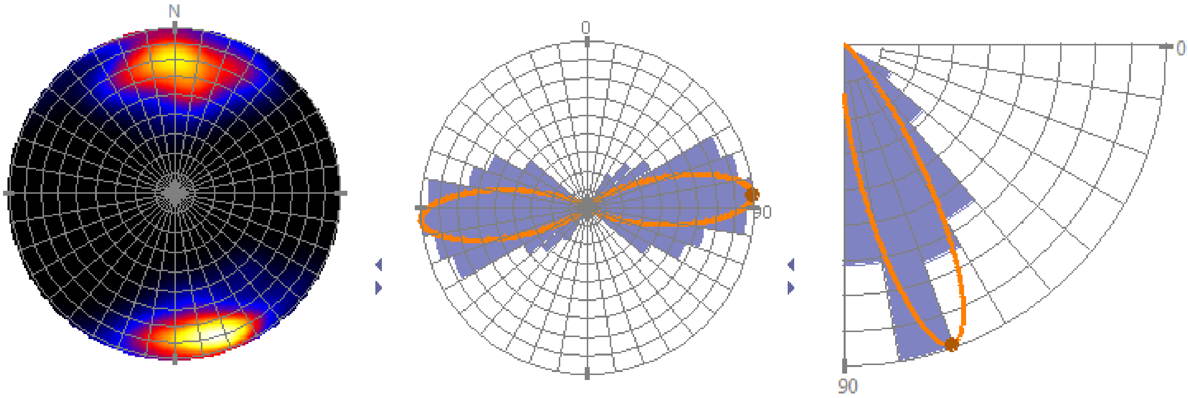

Figure 7 E-W fracture characteristics: fracture density (left), strike (center) and dip (right) diagrams with confidence ellipses for the population mean

The diffuse fracture families are then associated with the facies in terms of fracture densities as shown in Table 2. There is no fracture identified in the anhydrite facies but all the other facies exhibit some level of facture.

The estimated thickness of the various beds may be obtained from the density of the bedding fracture of the reservoir which is about 1 m for the limestone and dolomite. The parameters for size distribution, aperture, and conductivity are fairly uncertain and poorly constraint at this stage. The conductivity will be matched on the available well test.

Table 2 Mean fracture density (Number of fracture /meter) as a function of facies.

Facies	E-W	N-S
Dolomite	0,32	0,98
Limestone	0,58	0,93
Marl	0,04	0,09
Shale	0,23	0,20
Anhydrite	0	0

Preprints (www.preprints.org) | NOT PEER-REVIEWED | Posted: 23 May 2018 doi:10.20944/preprints201805.0324.v1

Peer-reviewed version available at Geosciences 2018, 8, 354; doi:10.3390/geosciences8090354

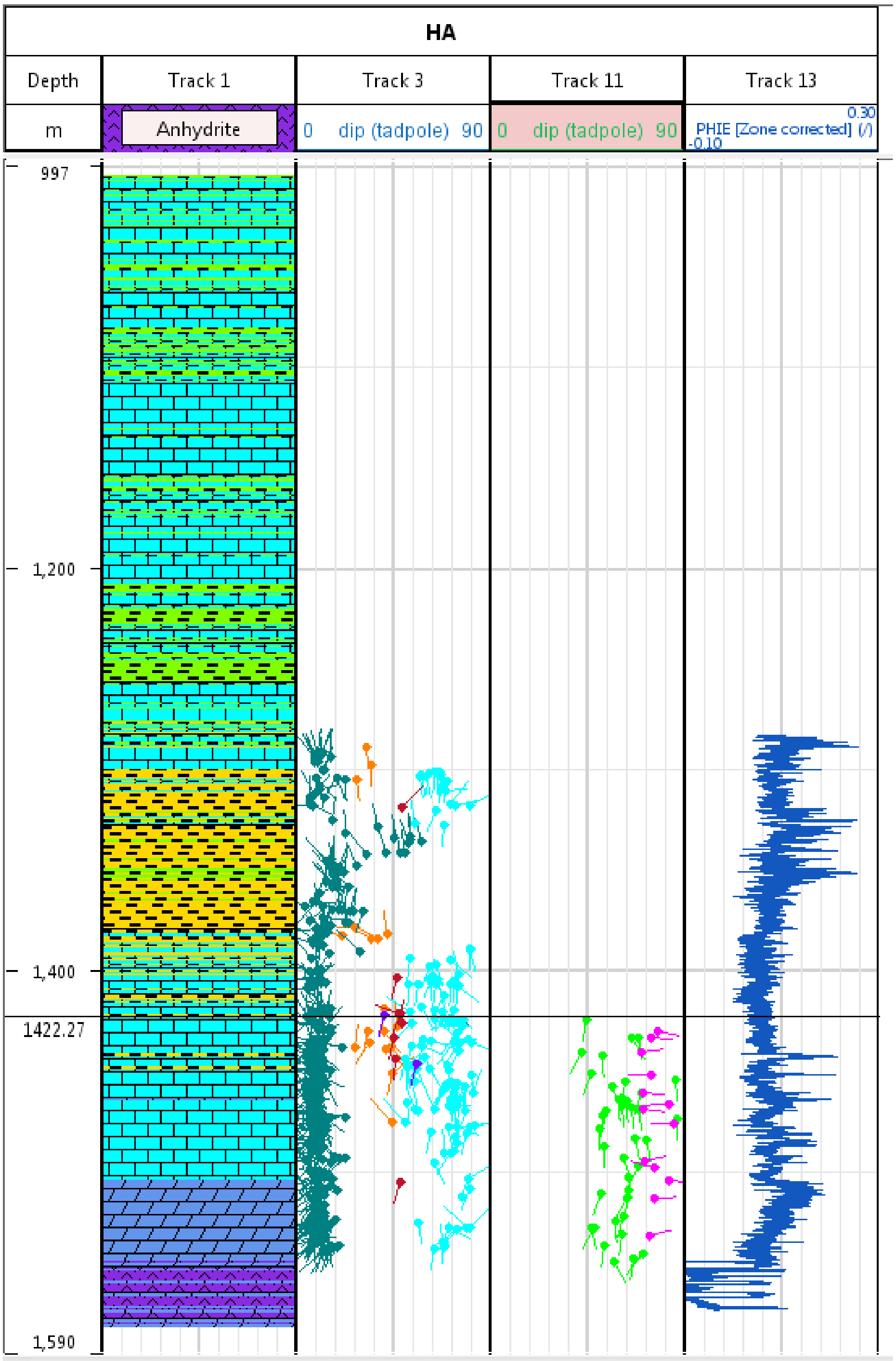

Figure 8 Facies, fracture dip (bedding in dark green), interpreted N-S (purple) and E-W (light green) fracture families and porosity logs for HA

DFN modeling

A DFN is a realization of the statistical model and is a 3D representation of the fracture model which includes the two families of identified fractures.

FracaFlow™ enables an "automated KH calibration" to calibrate the fracture model, in order for the model to be as close to reality as possible. Some of model parameters are indeed very uncertain (conductivity for example). This calibration is based upon the interpreted well test [Le Gallo et al, 2017]. The automated KH calibration is an analytical calibration of the DFN parameters on a well test interpretation. The algorithm will find the values of the conductivity

Peer-reviewed version available at Geosciences 2018, 8, 354; doi:10.3390/geosciences8090354

and eventually other parameter necessary to match the well test. This calibration is based on an analytical upscaling (Oda's formula: $K_{eq} = \sqrt{K_{min} * K_{max}}$). A DFN around HI limited to the Upper Calcareous Sopeña is used for the conductivity calibration.
The parameters considered in the automated KH calibration are the conductivity of E-W diffuse fracture, and conductivity of N-S diffuse fractures. In order for the calibration algorithm to converge a large enough number of initial solutions, i.e. greater than 500, must be computed. The results reported in Table 3 are computed for at least 1000 generations of the genetic algorithm which is significantly beyond the expected default convergence. The calibration is performed on Upper Calcareous Sopeña with the matrix properties described previously (see section Petrophysical model)

Table 3 Simulated conductivity in different fall-off for HI as reported by Le Gallo *et al* [2017].

	Interpreted Conductivity (K*H) (mD.m)	Simulated Conductivity (K*H) (mD.m)	E-W fracture conductivity (mD.m)	N-S fracture conductivity (mD.m)
June 2014	70	75,5	NC(*)	NC (*)
August 2014	115	114,7	1,1	0,8
October 2014	160	160,9	NC (*)	1,4
December 2014	155	155,5	NC (*)	1,3
March 2015	**247**	**245,9**	**0,5**	**2,4**

(*) NC: no convergence for a minimum fracture conductivity of 10^{-16} mD.m

As shown in Table 3, convergence of the algorithm was only obtained on the last of the well test for both diffuse fracture sets given the DFN generated, the random number used to generate the analytical calibration. This value will be used to validate the DFN properties based upon the Upper Calcareous Sopeña properties. The results obtained for the March 2015 test indicates that a horizontal anisotropy is generated by the diffuse fracture network: the horizontal anisotropy ratio is about 5 (Table 3) between North-South and East-West directions.
The automated KH calibration options of FracaFlow™ are designed for conventional fractured reservoirs. The computed conductivities of the fracture networks are very low and the analytical automated KH calibration does not converge. The computed conductivity of the DFN around both HI and HA wells are shown in Figure 9.

The final step is the upscaling of the DFN properties (fracture conductivities) over the whole model. Upscaling enables to calculate equivalent parameters linked to diffuse fractures (permeability, porosity, block dimensions) using an analytical upscaling method. Consequently, the fracture properties will be spread to all facies (except anhydrite) and all zones of the geological model. Equivalent properties are then be computed for the fracture media at the scale of the grid block while the matrix properties are not modified. The matrix properties are not altered.

Peer-reviewed version available at *Geosciences* **2018**, *8*, 354; doi:10.3390/geosciences8090354

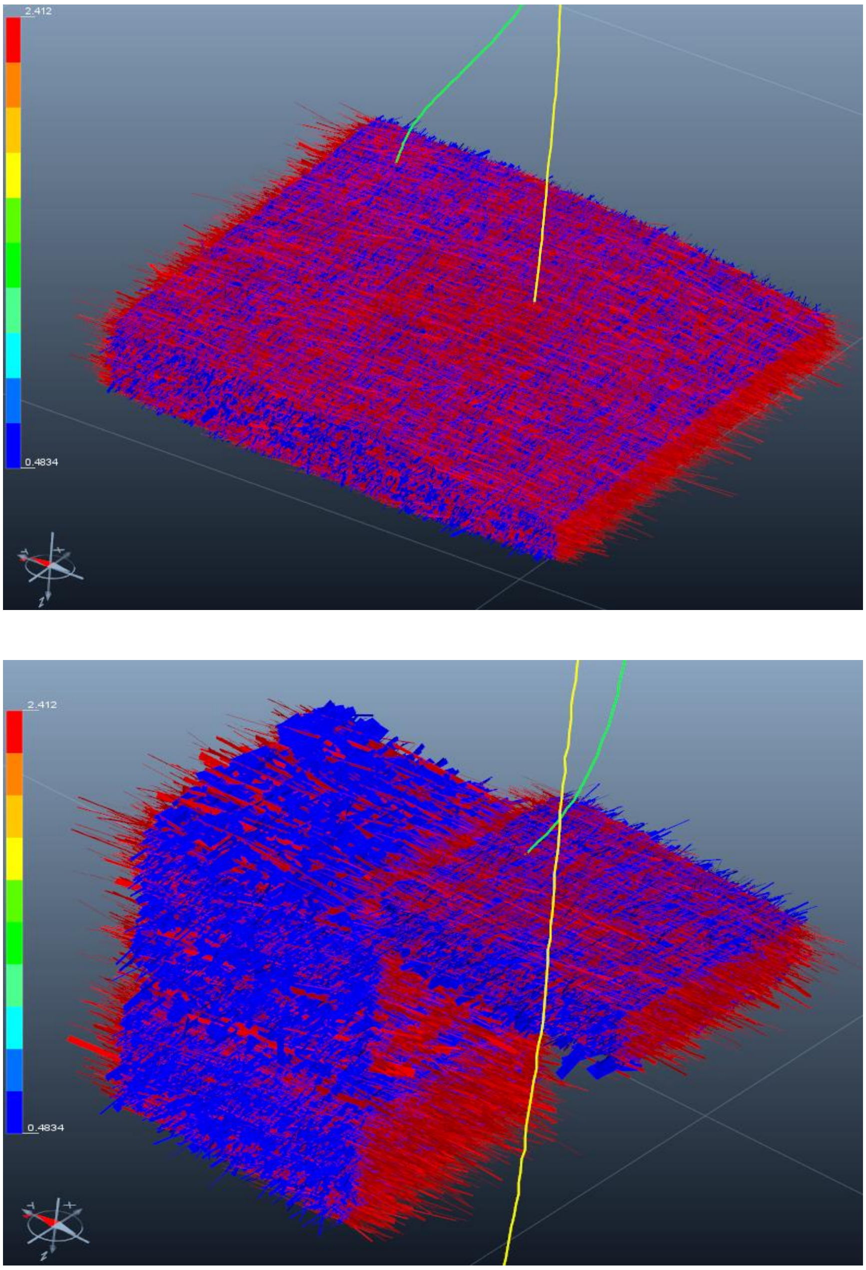

Figure 9 Calibrated conductivity (mD.m) of the E-W (blue) and in N-S (red) diffuse fracture networks in DFN around HI well in yellow (top) and HA well in green (bottom) in the storage formation

Conclusions and perspectives

A geological model encompassing the whole storage complex was established based upon newly-drilled wells, legacy wells and 3D seismic interpretation of the Hontomìn site. The matrix characteristics were mainly set from the newly drilled wells (HA the observation well and HI the CO_2 injection well) which were fully characterized by a complete suite of log acquisitions, laboratory works and hydraulic tests [de Dios et al, 2017]. The model major improvement is the integration of the diffuse fractures. Most of facies within the reservoir were fractured and two main families of fracture could be identified from the available log. The conductivities of the fracture networks are calibrated on the interpreted injection tests by matching their characteristics such as conductivity and aperture at the DFN scale, and subsequently they were upscaled to reservoir level and included to the geological model.

Peer-reviewed version available at *Geosciences* **2018**, *8*, 354; doi:10.3390/geosciences8090354

This model of the storage complex of the Hontomìn will later be used as a basis for the history matching of the dynamic model for the injections planned in ENOS project and in subsequent works to be conducted on site.

Acknowledgements

The authors acknowledge EU Horizon 2020 Program as funding party of ENOS project under Grant Agreement No 653718.

Sole responsibility lies with the authors, so the European Commission is not responsible for any use that may be made of the information contained in this article

References

Ali, A. M., Kumar, K., Murty, C. R., Lemaux, T., Ranjan, A., Dejoussineau, G., Bertrano, Ch., and Behira, H. (2009). Integrated reservoir connectivity study of Ahmadi fractured reservoir in Bahrain Field. SPE 120665. In *SPE/EAGE Reservoir Characterization & Simulation Conference*.

Alcalde, J., Marzán, I., Saura, E., Martí, D., Ayarza, P., Juhlin, C., Pérez-Estaún, A., and Carbonell, R. (2014). 3D geological characterization of the Hontomín CO_2 storage site, Spain: Multidisciplinary approach from seismic, well-log and regional data. *Tectonophysics*, 627, 6-25.

Bennion, D. B., Bachu, S. (2007). Permeability and relative permeability measurements at reservoir conditions for CO2-water systems in ultra-low permeability confining cap rocks. In *EUROPEC/EAGE Conference and Exhibition*. Society of Petroleum Engineers. SPE 106995

Bourbiaux, B., Basquet, R., Daniel, J.M., Hu L.Y., Jenni, S., Lange, A., and Rasolofosaon, P. (2005). Fractured reservoirs modelling: a review of the challenges and some recent solutions. First Break, v. 23, 33–40.

Cacas, M. C., Ledoux, E., Marsily, G. D., Tillie, B., Barbreau, A., Durand, E., Feuga, B., and Peaudecerf, P. (1990). Modeling fracture flow with a stochastic discrete fracture network: calibration and validation: 1. The flow model. *Water Resources Research*, *26*(3), 479-489.

Chadwick, A., Arts, R., Bernstone, C., May, F., Thibeau, S., andF Zweigel, P. Eds.(2008). Best Practice for the Storage of CO_2 in Saline Aquifers-Observations and Guidelines from the SACS and CO2STORE projects (Vol. 14). British Geological Survey.

Collier, H., Ridder, M., (1992). Utilization of the borehole televiewer in fracture analysis. Ground Water Manage. 13, 765–779.

Delprat-Jannaud F, Pearce J, Akhurst M, Nielsen CM, Neele F, Lothe A, Volpi V, Brunsting S, Vincké O. (2015).SiteChar - methodology for a fit-for-purpose assessment of CO_2 storage sites in Europe. Oil & Gas Science and Technology 70(4):531-554.

Dávila, G., Luquot, L., Soler, J. M., and Cama, J. (2016). Interaction between a fractured marl caprock and CO2-rich sulfate solution under supercritical CO_2 conditions. *International Journal of Greenhouse Gas Control*, 48, 105-119.

Peer-reviewed version available at Geosciences 2018, 8, 354; doi:10.3390/geosciences8090354

de Joussineau, G., Barrett, K. R., Alessandroni, M., Le Maux, T., and Leckie, D. (2016). Organization, flow impact and modeling of natural fracture networks in a karstified carbonate bitumen reservoir: an example in the Grosmont Formation of the Athabasca Saleski leases, Alberta, Canada. *Bulletin of Canadian Petroleum Geology*, *64*(2), 291-308.

de Dios J.C., Delgado M.A., Marín J.A., Martinez C., Ramos A., Salvador I., Valle L. (2016) Short-term effects of impurities in the CO_2 stream injected into fractured carbonates. *International Journal of Greenhouse Gas Control*, 54, 727-736

de Dios, J. C., Delgado, M. A., Martínez, C., Ramos, A., Álvarez, I., Marín, J. A., and Salvador, I. (2017). Hydraulic characterization of fractured carbonates for CO_2 geological storage: Experiences and lessons learned in Hontomín Technology Development Plant. *International Journal of Greenhouse Gas Control*, 58, 185-200.

Deflandre, J. P., Estublier, A., Baroni, A., Daniel, J. M., and Adjémian, F. (2011). In Salah CO_2 injection modeling: a preliminary approach to predict short term reservoir behavior. *Energy Procedia*, *4*, 3574-3581.

European Parliament Resolution of 14 January 2014 on implementation report 2013: developing and applying carbon capture and storage technology in Europe (2013/2079(INI)). Bullet 17.

Iding, M., Ringrose, P. (2010). Evaluating the impact of fractures on the performance of the In Salah CO_2 storage site. *International Journal of Greenhouse Gas Control*, *4*(2), 242-248.

Jing, L. (2003). A review of techniques, advances and outstanding issues in numerical modelling for rock mechanics and rock engineering. *International Journal of Rock Mechanics and Mining Sciences*, 40(3), 283-353.

Kovács, T. (2014). Characterization of the Hontomín reservoir and seal formations. Proceedings of the 4th Spanish-French Symposium on CO_2 Geological Storage.

Kovacs, T., Poulussen, D. F., and de Dios, J. C. (2015). Strategies for injection of CO_2 into carbonate rocks at Hontomin. GCCSI Final Technical Report. 66 pages

Le Gallo, Y., de Dios, J. C., Salvador, I., and Acosta Carballo, T. (2017). Dynamic characterization of fractured carbonates at the Hontomín CO_2 storage site. In *EGU General Assembly Conference Abstracts* (Vol. 19, p. 3468).

Ray, D. S., Al-Shammeli, A., Verma, N. K., Matar, S., De Groen, V., De Joussineau, G., Le Maux, T., and Al-Khamees, W. (2012). Characterizing and modeling natural fracture networks in a tight carbonate reservoir in the Middle East: A methodology. Bulletin of the Geological Society of Malaysia, 58.

Ringrose, P. S., Roberts, D. M., Gibson-Poole, C. M., Bond, C., Wightman, R., Taylor, M., Raikes, S., Iding, M., and Østmo, S. (2011). Characterisation of the Krechba CO_2 storage site: Critical elements controlling injection performance. *Energy Procedia*, *4*, 4672-4679.

Peer-reviewed version available at *Geosciences* **2018**, *8*, 354; doi:10.3390/geosciences8090354

Rubio, F.M., Garcia, J., Ayala, C., Rey, C., García Lobón, J.L (2014). Gravimetric characterization of the geological structure of Hontomín. In: 8a Asamblea Hipano-Lusa de Geodesia y Geofísica, Évora (Portugal), 29–31 January 2014.

Whittaker, S., Rostron, B., Hawkes, C., Gardner, C., White, D., Johnson, J., Chalaturnyk, R. and Seeburger, D. (2011). A decade of CO2 injection into depleting oil fields: monitoring and research activities of the IEA GHG Weyburn-Midale CO_2 Monitoring and Storage Project. Energy Procedia, 4, 6069-6076.

Glossary

DFN.- Discrete Fracture Network

ENOS.-Enabling Onshore CO_2 Storage in Europe

EP.- European Parliament

HA.- Hontomín auscultation well

HI.- Hontomín injection well

H2020.- European Horizon 2020 Research Programme

ICTJA.- Instituto de Ciencias de la Tierra Jaume Almera

K.-Permeability

KH.-Transmissivity

PDF.- Probability Distribution Fonction

TDP.- Technology Development Plant